Design of VSC Connected Low Frequency AC Offshore Transmission with Long HVAC Cables

Jonathan Ruddy, *Student Member, IEEE,* Ronan Meere, *Member, IEEE,* Cathal O'Loughlin, *Member, IEEE,* and Terence O'Donnell, *Member, IEEE*

***Abstract*—Low Frequency AC transmission (LFAC) has been proposed as an alternative to High Voltage DC transmission for medium distance (80-150 km) offshore wind farms. Long HVAC cables and their associated low frequency resonance, connected to Voltage Source Converters (VSC) provide technical challenges for the control of the offshore voltage. This paper provides the design of the offshore voltage 'grid forming control', to maintain a stable offshore voltage accounting for the connection of a long HVAC cable connected to the VSC. Simulations are performed on a LFAC test system to examine the influence of controller parameters and the associated design trade offs between the selection of *dq* controller time constants and voltage control bandwidth. The LFAC system design and control is then validated in a hardware experiment where the proposed controller operates in a real time, hardware in the loop experiment.**

***Index Terms*—Low Frequency Transmission, Voltage Source Converters, Converter Control, HVAC Cable Resonance.**

I. Introduction

THE development of offshore wind has increased recently with a view towards creating a suite of clean and sustainable energy sources. Consequently there has been a significant drive in research and industry to improve the competitiveness of offshore wind compared to other energy sources. A major challenge with any offshore wind system is the deployment of power electronics in harsh offshore environments. Since one of the main aspects of competitiveness is the reliability of an energy source, there has been a change in the mindset of industry recently to minimize the complexity of offshore assets, with the aim of providing adequate reliability. The industry standard for connecting wind farms from far offshore is Voltage Source Converter (VSC) High Voltage Direct Current (HVDC). HVDC transmission requires an offshore VSC converter station to convert to DC for power transmission. This converter station is large and expensive to build and particularly to maintain. As an alternative, Low Frequency AC (LFAC) transmission has been proposed [1]. AC cables operated at a lower frequency have a lower charging current compared to a cable operated at 50 Hz. This extends the distance which AC power can efficiently be transmitted from up to 100 km with compensation for HVAC cables at 50 Hz to 200-250 km with LFAC at 16.7 Hz [2]. A review of the research has shown that LFAC transmission is a competitive transmission option for offshore wind farms between 100 km and 200 km from shore [3]. LFAC uses AC transmission with proven AC components where expertise from onshore AC systems can be utilized in offshore transmission systems. The key advantage over HVDC transmission is the removal of the offshore converter station. Instead the frequency converter is located onshore to convert from LFAC at 16.7 Hz to the grid frequency.

For an LFAC system, a number of options exist for the choice of frequency converter. Using a cycloconverter to directly convert from low frequency to grid frequency is an option which has been widely discussed [4], [5]. Direct AC-AC conversion with a cycloconverter is difficult to achieve from low frequency to a higher frequency, leading to high levels of low order harmonics which require large filters [6]. It has been suggested that the most appropriate frequency converter is a back to back (BtB) VSC based converter [1], [7], [8] due to the independent controllability of active and reactive power,the de-coupling effect of the DC-link and the ability to establish offshore grid voltage and frequency. Modular Multi-level Matrix converters (MMxC) have also been proposed [9], which have the ability to perform direct AC-AC conversion with control over active and reactive power. However despite extensive research the MMxC has achieved a very low market penetration compared to BtB converters [10]. BtB converters, cycloconverters and MMxC have been reviewed and compared for LFAC transmission in [3]. Modular Multi-level Converter (MMC) designs for LFAC were considered in Tang *et al.* [8]. Although the MMC has lower losses and smaller inductive filtering requirement it was found that each capacitor module is required to be 3 times the size a similar MMC operating with a 50 Hz system, contributing to extra costs and footprint of the onshore station. It is proposed in this paper to use a 2 level converter to model the BtB converter, to avoid this extra cost and footprint onshore. In reality an extensive study on the trade-off between the cost of higher switching losses over time and the cost of the larger MMC converter is required, however such a study outside of the scope of this paper. The contribution of this paper is the design and application of the outer voltage controller in LFAC transmission, which is used in conjunction with MMC control [11] or 2-level converter control [12]. A MMC converter could be used on the grid side of the BtB converter if desired to connect to the 50 Hz

This work was conducted in the Electricity Research Centre, University College Dublin, Ireland, which is supported by the Electricity Research Centre's Industry Affiliates Programme (http://erc.ucd.ie/industry/). This material is based upon works supported by the Science Foundation Ireland and is funded through the SEES Cluster, under Grant No. SFI/09/SRC/E1780. The opinions, findings and conclusions or recommendations expressed in this material are those of the author(s) and do not necessarily reflect the views of the Science Foundation Ireland.

J. Ruddy, C. O'Loughlin and T. O'Donnell are with the School of Electrical and Electronic Engineering, University College Dublin, Dublin 4, Ireland; e-mail: jonathan.ruddy@ucdconnect.ie; terence.odonnell@ucd.ie.

R. Meere is with ESB Networks, Ireland

system, allowing the BtB converter the advantages of MMC technology while reducing costs and complexity on the low frequency side.

The VSC on the low frequency side is required to establish and maintain the offshore low frequency voltage. AC cables have a resonant frequency associated with the capacitance and inductance of the cable. LFAC will involve the connection of long cables to the AC side of the VSC, unlike HVDC where the cable is connected to the DC side. Therefore resonance interactions between the cable and the LFAC filter may be a concern. Moreover, at low frequency the filter components will be larger than they would in a 50 Hz system.

The combination of the large filter inductance and the cable capacitance has the impact of moving the resonant frequency of the combined filter and cable system to lower frequencies. This effect has been seen before in previous publications on LFAC transmission, Canelhas *et al*. [13] found that for a 200 km transmission cable and BtB converter system the resonant frequency was close to 50 Hz. Large damping filters were used to maintain transmission system stability. These filters are both large and expensive and can have significant (losses 1-2%) and consume a large portion of reactive power (50-70% of power). With resonant frequencies below the 14^{th} harmonic inductive elements may interact with the resonance to cause temporary over-voltages (TOV) if there is a disturbance on the system [14], [15]. TOVs cause instability in the voltage which the low frequency side converter is attempting to control. A sustained TOV will cause offshore breakers to trip resulting in disconnection from the onshore system. For any long HVAC cable connected to the onshore system these issues are prevalent. In HVAC (50 Hz) transmission, the offshore wind farm is connected directly to the onshore grid, meaning disturbances are propagated to the onshore system. Conversely in LFAC transmission, the cable is connected to a BtB VSC which decouples the cable from the onshore grid. It is important to analyze the interactions between the cable, the filter and the VSC control and compensate for any issues present with filtering or proper VSC controller design.

The key contributions of this paper are as follows: The characterization of the impact of connecting a long LFAC cable to a VSC and filter system. The application of an adapted VSC voltage control scheme for the connection of long HVAC cables to maintain a stable offshore voltage in an LFAC transmission system. The characterization of the design trade offs between switching frequency, filter capacitance and controller parameters to minimize the amplitude and duration of TOV's, and hardware based verification of the LFAC transmission system design with a BtB converter onshore. The paper is laid out as follows. Section II describes the issue of HVAC cable resonance. The LFAC system design is outlined in Section III. Section IV describes the common voltage control scheme for a VSC. Section V examines the addition of a HVAC cable to the voltage control loop, examining the frequency responses of the system to design an adapted voltage controller compensator. In section VI simulations are conducted to analyze different controller parameters in terms of system stability and response to TOV's. This approach is then validated in Section VII on a scaled hardware model of the LFAC transmission system, with the control operating in real time through a hardware in the loop real time simulation.

II. HVAC cable Resonance

The introduction of a long transmission cable adds a large capacitance, which depending on cable length can create low frequency resonance issues. The longer the cable, the lower the frequency of the over-voltage associated with the cable system, due to its large charging capacity. Low frequency resonances are often poorly damped [16] and can cause over-voltages to exceed insulation strength of many devices, causing failures and interruption of supply [17]. It is important to note that since there are no loads offshore, resonances are less damped than in onshore grids. Traditional designs of control for converters consider the grid they are connected to as a lumped inductance and neglect the impact of the connected HVAC cable, however this large capacitance cannot be neglected. Zhang *et al.* [18] consider the impact of long HVAC cables on the control of the Wind Turbine Generator (WTG) converter, proposing a new grid modelling method and control architecture to deal with high frequency resonances. In the LFAC case the WTG are connected via a HVAC cable to a large VSC, therefore no synchronous grid is present. The VSC is responsible for establishing and maintaining stability of the offshore grid. VSC's can become unstable dues to series resonances which are caused by HVAC cables. In [19] the authors have examined the impact of the VSC controller parameters on system stability, given the connection of different lengths of HVAC cable. They only considered the impact of adding cables up to 100 km in length. LFAC cables have the capability to reach up to 250 km, further increasing the problem with low frequency resonance. This low frequency resonance is a problem for LFAC voltage control stability and ability to control TOV's [7].

III. LFAC offshore system design

This section describes the layout of an offshore wind farm connected via LFAC transmission displayed in Fig. 1. It comprises an offshore wind farm where the converters of the wind turbines are configured to output 16.7 Hz AC voltage [20], these wind turbines are connected to a low frequency collector network. For the wind turbines to produce lower frequency a low frequency transformer is required in the nacelle of the wind turbine. One disadvantage of LFAC is that the transformers and inductors will be larger than the 50 Hz equivalent, however with appropriate transformer design it is possible to limit this increase in size to 77% compared to 50 Hz [21]. On the offshore platform a LFAC transformer increases the voltage from the collection network voltage to the LFAC transmission voltage. The wind farm is connected to shore via a HVAC transmission cable, which is operated at 16.7 Hz. An LC filter is employed at the connection point onshore to ensure a stable offshore grid voltage. A BtB converter is utilized to change the frequency from low frequency to the onshore grid frequency. The critical advantage of LFAC over HVDC is the removal of the offshore converter station, and placing a BtB converter onshore. This

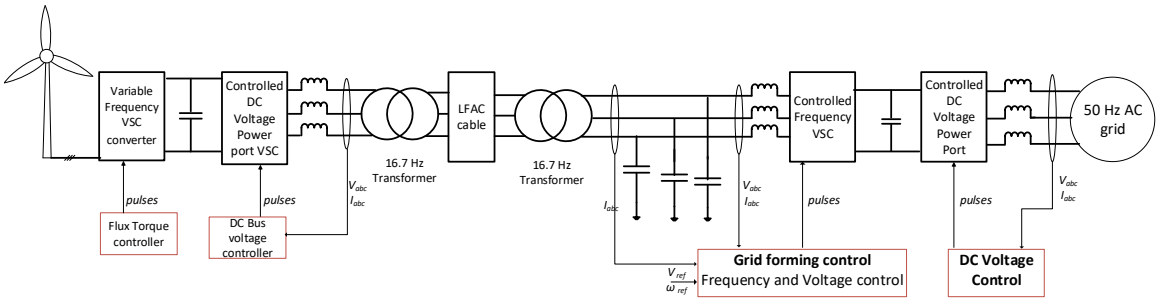

Fig. 1: LFAC transmission system.

has significant advantages in terms of installation costs and particularly operation and maintenance costs of the converter stations [7].

A. High level control functions

The offshore wind turbine converters synchronize via a phased locked loop (PLL) to the offshore grid which has been initialized by the BtB converter onshore. Control of the onshore BtB converter is pivotal to the control of the transmission system. Fig. 1 displays the high level control functionality required for each converter and for the converter system at the wind turbine. The BtB converter comprises two VSCs; a controlled frequency VSC connected to the LFAC cable required to establish and maintain the low frequency AC voltage magnitude and frequency with a grid forming control scheme, and a controlled DC power port VSC connected to the onshore 50 Hz power system which maintains a constant DC voltage. The control of the DC power port VSC consists of an inner current controller and DC bus voltage controller. These are designed following the techniques outlined in [12]. The DC bus voltage controller maintains the DC voltage at a constant value and provides reference signals to the inner current control scheme, which determines the reference voltage signal for the Pulse Width Modulation (PWM) switching which controls the IGBT VSC switches.

B. Grid forming control for LFAC grid

The grid forming control is required to establish and maintain the offshore grid voltage frequency and magnitude. The controller must be able to operate in steady state conditions and in response to disturbance events. For example, sudden increases or decreases in power generation from the wind farm or sudden voltage changes. These disturbance events can excite the resonant frequency of the combined filter and cable system, causing the voltage to become unstable and trip protection. The objective of the voltage controller is to maintain stability and avoid tripping protection systems. Fig. 2 shows the control architecture of the grid forming controller. The control is adapted from a control strategy for islanded operation of a distributed resource unit in [22]. The objective of the control is to regulate the amplitude and frequency of the offshore voltage (V_{sdq}) in response to changes in the offshore current (I_{odq}). The voltage control block provides the reference currents for the *dq* current control scheme. Since there is no voltage for a PLL to lock onto, a virtual PLL provides a reference angle for the voltage controller and inner current controller to control the switching of the VSC at the desired frequency.

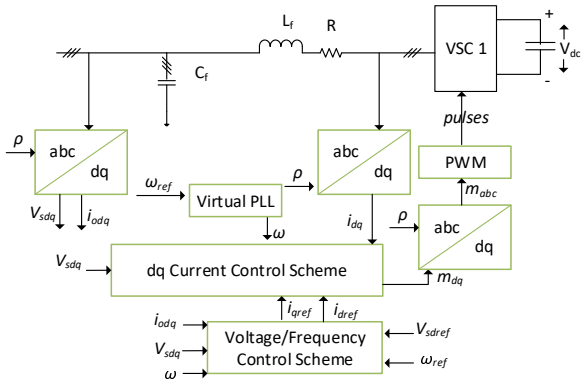

Fig. 2: Grid forming control on the LFAC side VSC to maintain the offshore voltage magnitude and frequency.

C. LC filter

Since the purpose of this work is to reduce the requirement for large AC filters to maintain stability, a simple LC filter is chosen for the offshore side of the BtB converter. The capacitance C_f is required in the LFAC grid to maintain a stable voltage and to filter switching current harmonics. The inductor L_f is required to eliminate the current ripple created by the VSC. The size of the inductor is commonly chosen to be between 0.1pu and 0.15pu [12]. Capacitor size is determined by:

$$f_r = \frac{1}{2\pi\sqrt{LC}} \tag{1}$$

The typical requirements of an LC filter are to have corner frequency (f_r) designed at between 10% and 20% of the switching frequency, minimize reactive power under rated conditions and minimize filter inductance voltage drop at rated current [18]. Increasing the converter switching frequency will increase the design corner frequency of the LC filter, reducing the size of the filter components. To reduce cost and economic footprint it is prudent design to reduce the size of these filters where possible because a main disadvantage of LFAC transmission is that the inductive filter components are three times larger than at 50 Hz [1].

IV. VSC Voltage Controller Design

The voltage control block in Fig. 3 inputs a reference *dq* voltage, which is compared to the measured *dq* voltage at the capacitor of the LC filter. An output reference current is added to a feed forward measurement to provide the reference i_{dq} for the *dq* current control scheme.

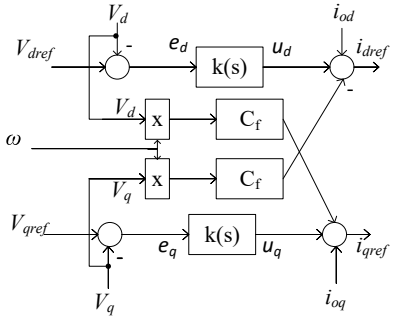

Fig. 3: Voltage control block.

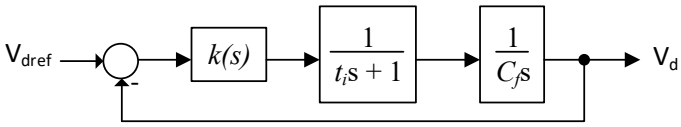

Fig. 4: Control block diagram of controlled frequency VSC.

Fig. 4 shows the *d* component small signal control block diagram of a controlled frequency VSC system. The same control loop exists for the *q* component. The plant is a representation of the closed loop response of the inner current controller, VSC and inductor dynamics designed so as to have a response time of t_i. The final block represents the capacitor dynamics. The plant has a pole at *s=0* and a real pole at $s = -t_i^{-1}$.

The design procedure for $k(s)$, the compensator transfer function, is based on the method in [22]. The compensator is designed to ensure a fast stable response and zero-steady state error and to have adequate bandwidth and stability to avoid disturbance inputs causing voltage instability.

Let the compensator $k(s)$ be given by:

$$k(s) = k\frac{s+z}{s} \tag{2}$$

where *k* and *z* are the compensator gain and zero. Then, the loop gain is described in Eqn. 3, indicating a double pole at $s = 0$. This causes $\angle l(j\omega) = -180^\circ$ at low frequencies.

$$l(s) = \frac{k}{t_i C_f}\left(\frac{s+z}{s+t_i^{-1}}\right)\frac{1}{s^2} \tag{3}$$

Assuming $z < -t_i^{-1}$ the open loop phase reaches its maximum (δ_m) at the frequency $\omega = \omega_m$. To obtain the maximum phase margin available the gain crossover frequency (ω_c) should be selected as ω_m. δ_m then becomes the phase margin which is selected as a design choice. z is then calculated by:

$$Sin(\delta_m) = \frac{\frac{t_i^{-1}}{z} - 1}{\frac{t_i^{-1}}{z} + 1} \tag{4}$$

The gain crossover frequency which determines the bandwidth of the controller is calculated by:

$$\omega_c = \sqrt{z t_i^{-1}} \tag{5}$$

The compensator gain *k* is obtained from the solution of letting the magnitude of $l(j\omega_c)$ equal to one, that is:

$$k = C_f \omega_c \tag{6}$$

V. Voltage controller design including HVAC cable

The HVAC cable affects the voltage at the filter capacitor, which has an impact on the control and stability of the system. If the controller is not designed to compensate for the effect of the long AC cable, then the voltage may not be stable and controlled.

TABLE I: LFAC transmission cable data at 50 Hz.

Voltage (kV)	R (Ω/km)	X (Ω/km)	C (nF/km)
220	0.046	0.07	198

In order to determine the resonant points of the LFAC transmission system a frequency sweep from 1 to 2000 Hz is performed on the VSC connected to the LC filter and HVAC cable [15]. Tab. I shows the cable parameters used with a filter inductance and capacitance of 85.8 mH and 4.03 μF. Fig. 5 displays the frequency sweep for 150 and 300 km HVAC cables. Distributed parameter or multiple pi cable models are the most accurate representation for long cables, particularly at high frequencies. To obtain the lower frequency resonant points of the system, the cables are modelled using 5 pi-sections. The low frequency peaks represent the LC resonance of the filter which has been moved to a lower frequency by the presence of the cable. The LC resonance is designed to be 270 Hz, however the addition of the cable capacitance reduces this resonance to 88 Hz and 62 Hz for 150 and 300 km cable lengths.

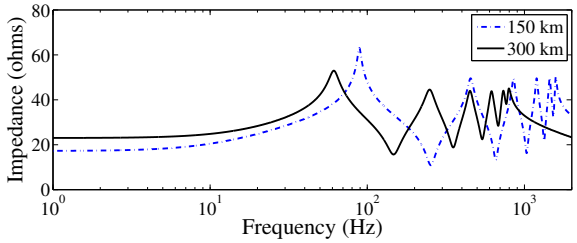

Fig. 5: Resonant peaks of 220 kV cable combined with LC filter.

These low frequency resonances have the potential to provide significant difficulties in terms of maintaining stability and sustaining harmonic levels below an allowable threshold if the controller is not appropriately designed. From a voltage control compensator design point of view, analysis of the open loop system is performed using a lumped pi model. Using a

single pi section to model the cable will accurately represent the first filter LC resonance and the first cable resonance. These are the resonant points of interest for voltage control stability.

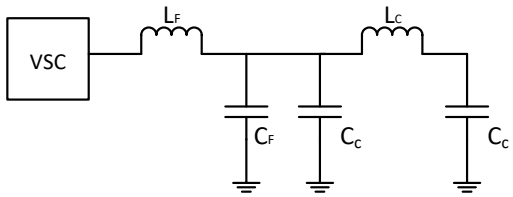

Fig. 6: VSC connected to filter and cable.

Fig. 6 shows the layout of the pi cable model connected to the LC filter and VSC. The voltage at the filter capacitor is dependent on the current drawn by the parallel combination of the filter capacitor and the cable equivalent capacitance. Since the cable has an impact on the voltage measured it impacts the structure of the control block diagram, illustrated in Fig. 7.

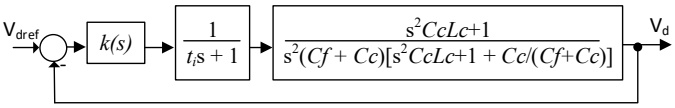

Fig. 7: Control block diagram including LFAC cable.

It follows that Eqn. 7 describes the open loop gain of the controlled frequency VSC system including the cable in the small signal model.

$$l(s) = \frac{k}{t_i(C_f + C_c)}\left(\frac{s+z}{s+t_i^{-1}}\right)\left(\frac{s^2C_cL_c+1}{s^2[s^2C_cL_c+1+\frac{C_c}{C_f+C_c}]}\right) \tag{7}$$

The introduction of the HVAC cable adds a double pole and double zero to the open loop system resulting in the dip and peak in the loop response. The cable capacitance in the open loop system will reduce the magnitude of the frequency response, reducing the voltage controller crossover frequency to below ω_m, therefore reducing the phase margin to some value below the selected δ_m.

In order to illustrate the issues with controlling the LFAC voltage while connecting a HVAC cable, the compensator is first designed using the voltage control compensator in Eqn. 6. In this analysis the cable parameters in Tab. I are used, with filter inductance and capacitance of 85.8 mH and 4.03 μF respectively and the control parameters t_i and δ_m set to 1 ms and 53°. Fig. 8 shows the open and closed loop frequency response of Fig. 7 with the addition of different cable lengths from 50 km to 300 km. This response incorporates one pi-section cable model. In the open and closed loop system the magnitude is continually decreasing as frequency increases, therefore the impact of extra pi-sections on the frequency response will be at negative magnitudes. The open loop frequency response for the case with no cable verifies a 53°phase margin at ω_c = 334 rad s^{-1} indicating that under these conditions the voltage controller will provide a stable response, verified in the closed loop plot. However, increased cable length reduces the crossover frequency below the desired value. It follows that at longer cable lengths, with reduced crossover frequencies and a reduced phase margin the closed loop response provides positive gains causing oscillations in the response of the controlled frequency VSC with a cable connected.

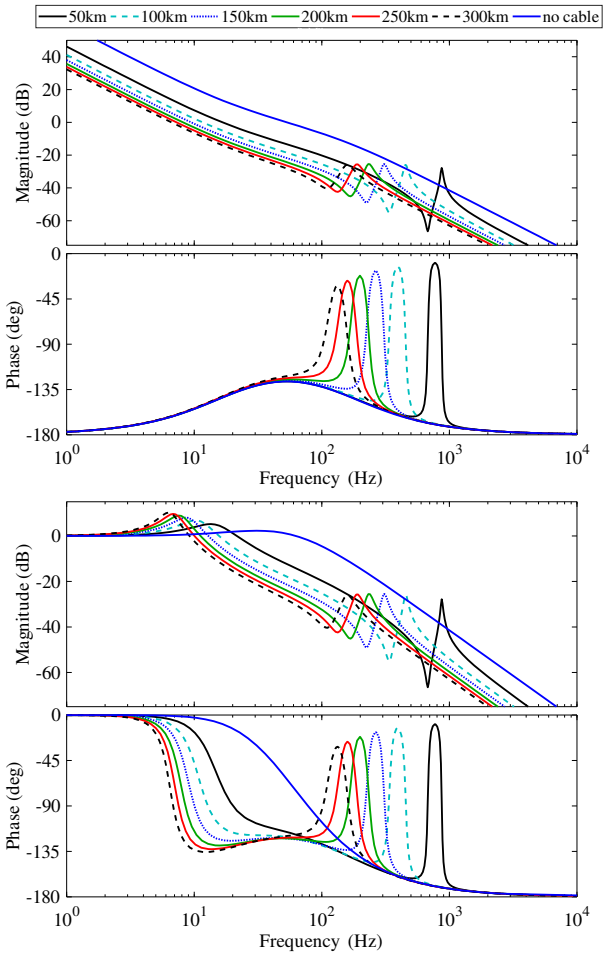

Fig. 8: Open loop and closed loop frequency response with cables from 50 km to 300 km.

To maintain the stability of the controlled frequency VSC system the controller gain *k* must compensate for the reduced magnitude of the frequency response with increased cable length. Reviewing Fig. 8, the range of the crossover frequencies is not impacted by the cable resonance which is due to the inductance and occurs at much higher frequencies. The cable capacitance has the effect of reducing the magnitude of the open loop plot. It is clear that to maintain the stability of the controlled frequency VSC system the controller gain *k* must compensate for the reduced magnitude of the frequency response with increased cable length. The cable capacitance drives the decrease in magnitude, and therefore the decrease in crossover frequency, in order to evaluate the compensator gain an open loop system without the cable inductance effect can be examined. This produces a loop gain defined by Eqn. 8. Since the cable inductance is neglected in this instance the loop gain

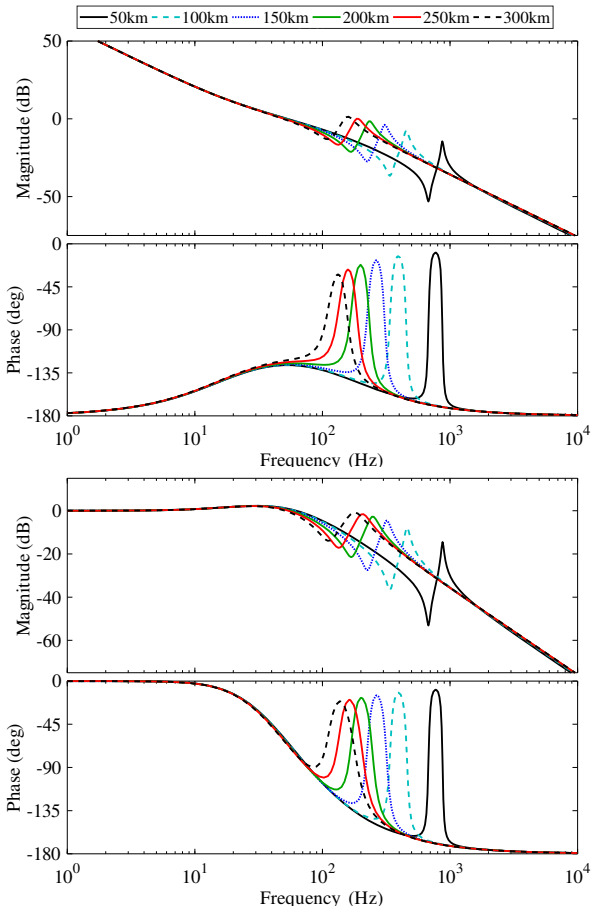

Fig. 9: Open and closed loop frequency response with updated controller for any cable length.

becomes similar to Eqn. 3 with the total cable capacitance and the filter capacitance added in parallel.

$$l(s) = \frac{k}{t_i(C_f + C)}\left(\frac{s+z}{s+t_i^{-1}}\right)\frac{1}{s^2} \tag{8}$$

Where C is the total cable capacitance. The gain crossover frequency (ω_c) is set by Eqn. 5 then the new compensator gain k is obtained from the solution of Eqn. 8, setting $l(j\omega_c) = 0$ Eqn. 9 yields the new compensator gain.

$$k = (C_f + C)\omega_c \tag{9}$$

Eqn. 9 is used to calculate the compensator gain value incorporating cable length. The open and closed loop response for any cable length is shown in Fig. 9. As required the phase margin is 53°and the crossover frequency is about 334 rad s^{-1}. This indicates that for any cable length, the voltage controller with a compensator designed as in Eqn. 9 will provide a closed loop response without significant positive gains. This modification to the controller design strategy will maintain the crossover frequency at the desired value for any length of LFAC cable, with the result that the controller will have the ability to reject disturbance inputs below the controller bandwidth. Although the plant (i.e. the cable plus filter system) does have an inherent disturbance associated with the cable resonance, the closed loop plot of Fig. 9 shows that the closed loop system is stable with the new compensator design for all cable lengths from 50km to 300 km. This analysis has been performed at a fixed power level with varying transmission distance. It is worth noting that increasing the power level for this analysis will lead to different LC filter and cable parameters, however the procedure to control the bandwidth will remain the same. To further improve the stability of the voltage control the bandwidth can be increased by varying design parameters.

From Eqns. (7) and (9) it can be seen that the bandwidth of the controller is dependent on the phase margin and on the time constant of the *dq* current control scheme (t_i) which dictates the placement of the real pole $-1/t_i$. The time constant (t_i) for standard VSC control is typically selected to be between 0.5 and 5 ms. However, the bandwidth of the inner current controller ($1/t_i$) must be considerably smaller than the switching frequency of the VSC [12]. The selection of the switching frequency is an interesting decision for an LFAC transmission system. Intuitively since the fundamental frequency is 3 times lower, the switching frequency of the VSC on the low frequency side may be lower than the standard for HVDC transmission, preserving the ratio between fundamental and switching frequency. This would reduce switching losses, however reducing the switching frequency decreases the maximum allowable ($1/t_i$), thereby reducing controller bandwidth. This constitutes a design trade off which can be summarized by Tab. II.

TABLE II: Trade offs associated with compensator design choices.

	Filter C	max t_i	PI bandwidth	Switch Losses	damping
f_{sw} ↑	↓	↑	↑	↑	-
δ_m ↑	-	-	↓	-	↑

Increasing the phase margin improves the damping of the system to changes in voltage. The phase margins of 45°and 53°are of particular interest because at 45°two poles form a complex conjugate pair, with a damping ratio of 0.707, and 53°which makes the two complex conjugate pairs coincide with the pole at ω_c and a damping ratio of 0.994. The 2 cable poles remain in the same position. Using a higher phase margin the damping ratio is increased to 1, however the associated reduction in bandwidth renders this increase impractical. In the context of TOV's a higher bandwidth will increase the speed of the controller in response to disturbances, thereby reducing the magnitude and duration of the TOV's.

VI. Simulation with Test System

The test system used in this paper models a 200 MW offshore wind farm connected via a 150 km, 220 kV LFAC cable. The BtB converter is connected at 100 kV and a low frequency transformer steps up to the cable voltage. Tab. III shows the parameters used in modelling the LFAC transmission system. Four different sets of compensator parameters are

tested, ensuring fast dq control with t_i of between 0.5 ms and 1 ms, and appropriate damping with δ_m of 45°and 53°. The switching frequency bandwidth is selected to be approximately 8 times the bandwidth of the dq controller, and a multiple of the fundamental frequency. Tab. IV displays the details of the 4 controllers examined.

TABLE III: Parameters for LFAC transmission system.

Parameter	Value
Filter Inductance (L_f)	85.8 mH
Filter Capacitance (C_f)	4.03 μF
R	0.27 Ω
V_{DC}	400 kV
Transformer Turns Ratio (n)	2.2:1
$V_{sd}ref$, $V_{sq}ref$	100 kV, 0 V
Switching Frequency (f_{sw})	See Tab. IV
Modulation Scheme	SPWM

TABLE IV: Controller specifications.

Contr-oller	f_{sw} (kHz)	dq time constant (t_i)(ms)	Phase Margin (δ_m) (°)	Bandwidth (rad s^{-1}) (ω_c)	Damping Ratio
A	2.1042	0.5	45	828.4	0.707
B	2.1042	0.5	53	669.2	0.994
C	1.6533	0.75	53	446.1	0.994
D	1.3527	1	53	334.6	0.994

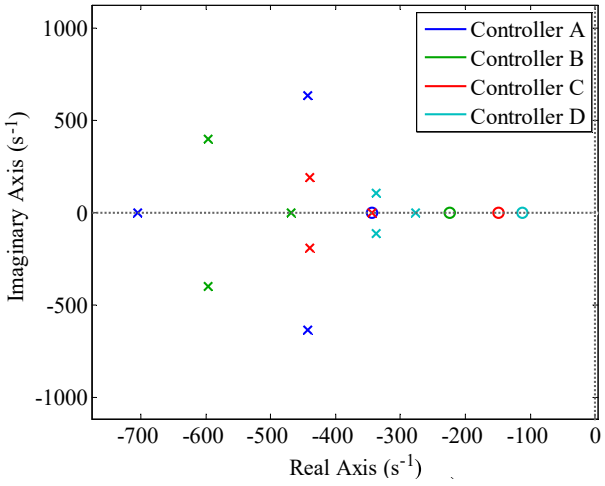

Fig. 10: Locations of poles and zeros for each controller.

Fig. 10 displays the locations of the closed loop poles and zeros on the voltage controlled VSC and cable system for each controller, further into the left half plane indicating increased stability. Fig. 10 does not include the cable poles which exist outside the limits of the y axis. Simulations are performed to examine each controller in the LFAC transmission test system. The gain of the voltage controller is calculated by Eqn. 9 where the cable capacitance (C) is transformed to the low voltage side of the LFAC transformer (where n is the turns ratio). The full switching simulations have been performed in Matlab Simscape Powersystems [23] modeling the LFAC offshore transmission system as depicted in Fig. 1. The cable is modelled in simulation using 5 pi-sections as in Fig. 5. Two tests are carried out to determine the appropriateness of the selected controllers.

1) After 0.5 seconds a voltage step is applied from 1 pu to 1.5 pu. The systems ability to respond to step changes in voltage depends both on the bandwidth and the phase margin of the compensator. Fig. 11 shows the response of each controller to this voltage step. As expected from Fig. 10 the controller with the largest bandwidth responds the fastest. Increased phase margin reduces the overshoot which can be seen in the difference between controller A and B.
2) After 1.5 seconds a power step from 0 to 0.5 pu is applied as a disturbance to the system. The objective of the controllers is to maintain the voltage at the desired value (1 pu) in response to the change in power.

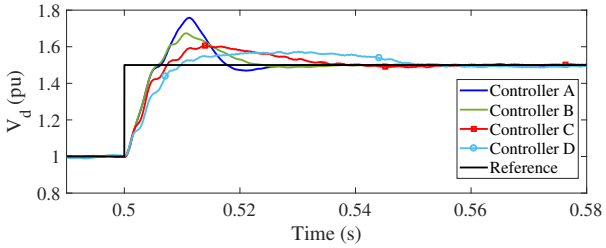

Fig. 11: V_d response to voltage reference step from 1 to 1.5 pu.

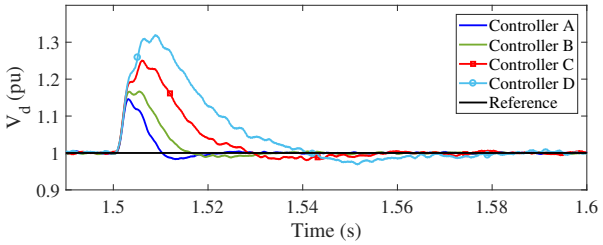

Fig. 12: V_d response to large current step.

Comparing the responses in Fig. 11 the response to a step change in voltage is quick and controlled, with the d component of the voltage returning to the reference value within 20-80 ms for the 4 controllers. This test verifies that the voltage control is stable when responding to a change in the LFAC voltage. In Fig. 12 the voltage controller is responding to an external disturbance, in this case a step increase in current to the controllers. It is clear again that the larger bandwidth controllers provide a more desirable response, responding in 20 - 40 ms to control the voltage. The TOV caused by the disturbance reaches as much as 1.3 pu for 20 ms for Controller D, which may cause stress and failure of protection equipment if not controlled back to the

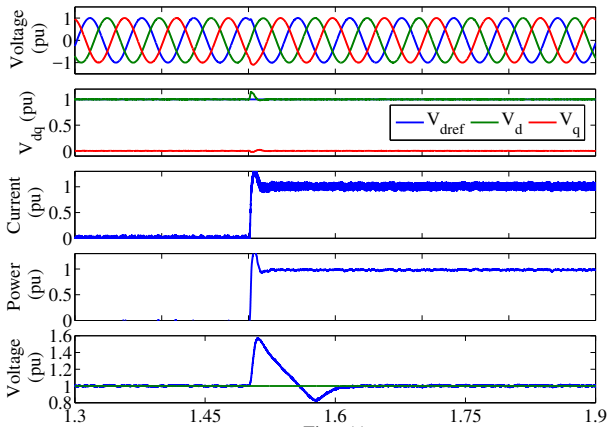

Fig. 13: Voltage, V_{dq}, Power transferred, I_d and V_{DC} from test system simulation for Controller A.

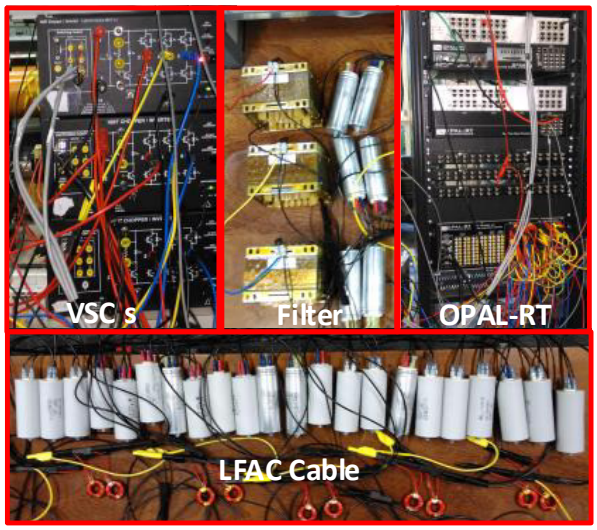

Fig. 14: Picture of hardware setup

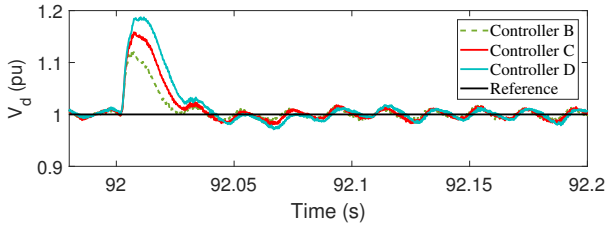

Fig. 15: V_d response to power step in hardware for three controllers.

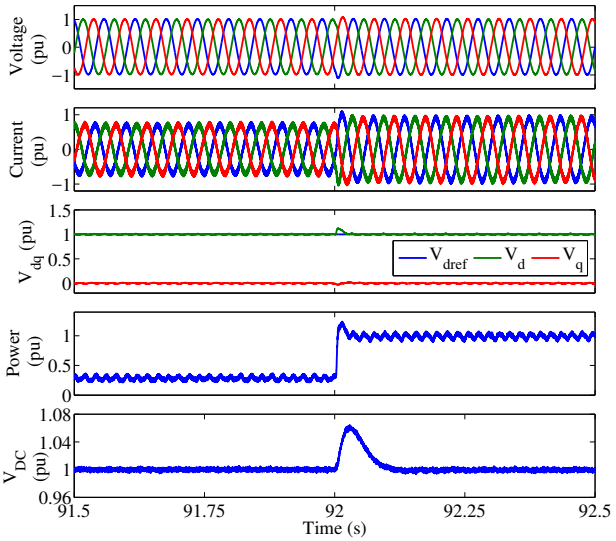

Fig. 16: LFAC Voltage, Current, V_{dq}, power and V_{DC} during step from 300 W to 1000 W.

reference value in time. TOV limits have been defined by the Irish transmission system operator on HVAC cables at 1.6 pu for the duration of one electrical cycle [24]. These results show each controller to be within this limit. For Controller A the TOV reaches almost 1.2 pu, returning after 20 ms to the desired value. Fig. 13 shows the LFAC voltage, power and the dq components of voltage and current using controller A which is the most stable of the studied controllers.

VII. Hardware Experimentation

To verify the design of the LFAC transmission system and the voltage controller design, the LFAC transmission system is built in hardware using the parameters in Tab. V. In hardware, the offshore wind farm is modelled as a DC source connected to the grid side converter of a wind turbine as shown in Fig. 17, with the control schemes operated in real time. This converter locks onto the 16.7 Hz grid produced by the BtB converter.

TABLE V: Parameters for scaled hardware LFAC transmission system.

Parameter	Value
Filter Inductance (L_f)	33 mH
Filter Capacitance (C_f)	80 μF
Cable Inductance (L_c)	9.21 μH/km
Cable Capacitance	4.79 μF/km
V_{DC}	500 V
$V_{sd}ref$, $V_{sq}ref$	100 V, 0 V
Switching Frequency (f_{sw})	1.3527 kHz
Voltage Controller Bandwidth (ω_c)	B: 669.2 rad s^{-1} C: 446.1 rad s^{-1} D: 334.6 rad s^{-1}

The BtB converter is comprised of two 2 kVA VSC's, with a 680 μF capacitor on the DC link. The cable is scaled using Eqn. 10 where k_{scale} is based on the ratio of the base impedance the hardware system and the real system [25].

$$k_{scale} = \frac{Z_{hardware}}{Z_{real}} = \frac{L_{hardware}}{L_{real}} = \frac{C_{real}}{C_{hardware}} \quad (10)$$

The experiment was performed with a 150 km scaled cable modeled with the total inductance and capacitance divided across 5 pi sections. Fig. 14 displays a picture of the hardware setup, including a single phase of the cable model. Fig. 15 shows the response of the voltage controllers B, C and D to

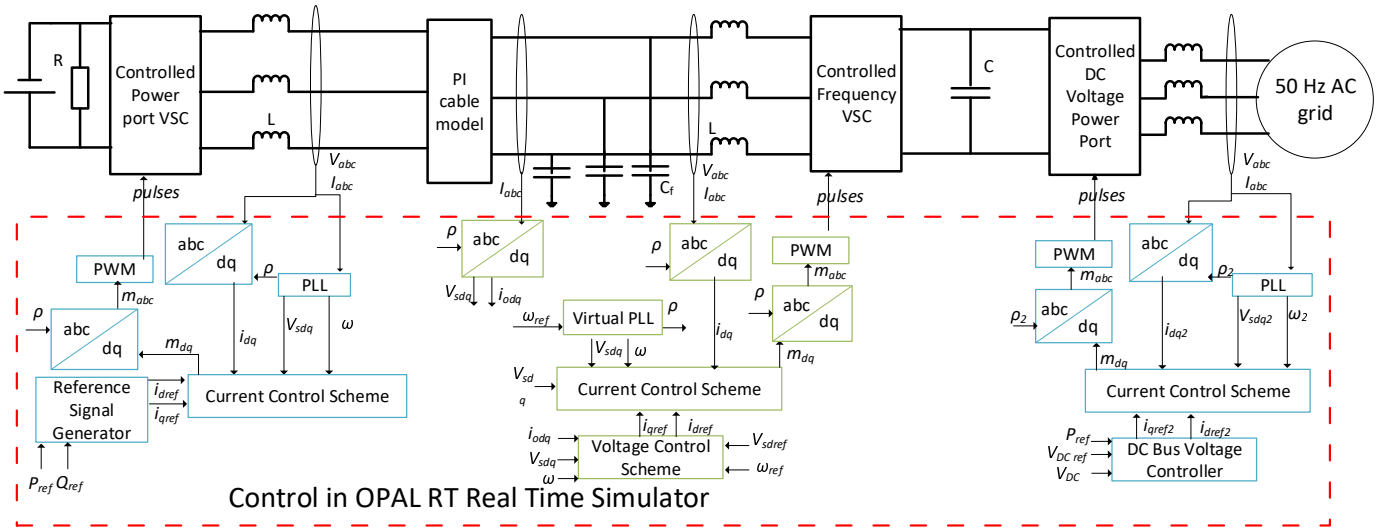

Fig. 17: LFAC transmission system hardware setup with OPAL RT real time simulator.

a 0.7 pu step in active power from 0.3 pu to 1 pu. It can be seen that Controller B provides the fastest and smoothest response as expected due to the increased ω_c, with controllers C and D responding as in simulation with a TOV of higher amplitude and longer duration (20 - 40 ms). The TOV's observed in hardware have lower amplitude than in the high power simulation. This is due to extra resistive damping in the hardware setup from the filter and cable implementations. The duration of the TOV's are similar to those in the simulation test, validating the controller design in hardware.

Fig. 16 displays the voltage, current, and power exported from the wind farm using Controller B, validating the overall LFAC system design and control in hardware. Comparing the hardware results to the simulation in Fig. 13 the same responses can be seen in the LFAC grid, validating the simulations. The DC link voltage responds much slower and has a smaller amplitude response than in simulation due to a much larger capacitor being placed in on the DC link in hardware.

VIII. Conclusion

This paper has presented the design and control of an LFAC transmission system with a focus on accounting for the impact of connecting a long HVAC cable operated at 16.7 Hz to a VSC. The addition of a long HVAC cable causes voltage control instability if the controller is not appropriately designed. The paper begins by presenting a VSC AC voltage control scheme which is adapted to compensate for the addition of a long HVAC cable. It can be seen that the adapted control strategy provides stable control of the LFAC system and different parameters are examined to reduce the magnitude of TOVs. The adapted PI control considers the impedance of the cable in the calculation of voltage controller gain to mitigate low frequency resonances caused by connection of a long HVAC cable. If resonances from the cable are still an issue, control of the LFAC voltage may be improved by use of a Proportional Resonant (PR) controller where the gain of the controller is depressed at the resonant frequency of the cable. Using this technique it is important to have good knowledge of the resonant frequencies. Recently techniques have been developed which could determine these through impedance measurements [26]. Although this work deals primarily with the stability of the LFAC voltage controller in the presence of the long transmission cable, it is also known from HVDC systems that harmonic interactions and sub-synchronous control interactions may occur between the voltage controlled VSC and/or the cable impedance and wind turbine output impedances [27]. To identify and avoid such issues, impedance analysis could be used to assess the stability of the system across the frequency range of interest, considering harmonic interactions and control interactions. Once frequency ranges of interest are determined the controller gains can be adapted to mitigate any issues. The proposed controller design is tested in simulation on an LFAC test system with various parameters accounting for design trade offs between controller time constants, phase margin and switching frequency. The design of the LFAC transmission system and the controller design have been validated in a hardware test setup. In this case the application is Low Frequency transmission, however, this paper provides an approach to design voltage controllers for any long HVAC cable connected to a controlled frequency VSC.

References

[1] W. Fischer, R. Braun, and I. Erlich, "Low frequency high voltage offshore grid for transmission of renewable power," in *3rd IEEE PES Innovative Smart Grid Technologies Europe*, Oct. 2012.

[2] R. Meere, J. Ruddy, P. Mc Namara, and T. ODonnell, "Variable AC transmission frequencies for offshore wind farm interconnection," *Renew. Energy*, vol. 103, pp. 321 – 332, 2017.

[3] J. Ruddy, R. Meere, and T. O'Donnell, "Low Frequency AC transmission for offshore wind power: A review," *Renew. Sustainable Energy Rev.*, vol. 56, pp. 75–86, 2016.

[4] H. Chen, M. H. Johnson, and D. C. Aliprantis, "Low-Frequency AC Transmission for Offshore Wind Power," *IEEE Trans. Power Del.*, vol. 28, no. 4, pp. 2236–2244, 2013.

[5] W. Xifan, C. Chengjun, and Z. Zhichao, "Experiment on Fractional Frequency Transmission System," *IEEE Trans. Power Syst.*, vol. 21, no. 1, pp. 372–377, 2006.

[6] J. Ruddy, R. Meere, and T. O. Donnell, "Low Frequency AC Transmission as an Alternative to VSC-HVDC for Grid Interconnection of Offshore Wind," in *IEEE PowerTech Eindhoven*, Eindhoven, 2015.

[7] E. Olsen, U. Axelsson, and A. Canelhas, "Low Frequency AC Transmission on large scale Offshore Wind Power Plants, Achieivng the best from two worlds?" in *13th Wind Integration Workshop*, Berlin, Germany, 2014.

[8] Y. Tang, P. B. Wyllie, J. Yu, X. M. Wang, L. Ran, and O. Alatise, "Offshore low frequency AC transmission with back-to-back modular multilevel converter (MMC)," in *11th IET Int. Conf. AC DC Power Transmission*, 2015, pp. 1–8.

[9] Y. Miura, T. Mizutani, M. Ito, and T. Ise, "Modular Multilevel Matrix Converter for Low Frequency AC Transmission," in *2013 IEEE 10th International Conference on Power Electronics and Drive Systems (PEDS)*, 2013, pp. 1079–1084.

[10] P. W. Wheeler, T. Friedli, J. W. Kolar, J. Rodriguez, and P. W. Wheeler, "Comparative Evaluation of Three-Phase AC AC Matrix Converter and Voltage DC-Link Back-to-Back Converter Systems," *IEEE Transactions on Industrial Electronics*, vol. 59, no. 12, pp. 4487–4510, 2012.

[11] U. N. Gnanarathna, A. M. Gole, and R. P. Jayasinghe, "Efficient modeling of modular multilevel hvdc converters (mmc) on electromagnetic transient simulation programs," *IEEE Transactions on Power Delivery*, vol. 26, no. 1, pp. 316–324, Jan 2011.

[12] A. Yazdani and R. Iravani, *Voltage-Sourced Converters in Power Systems Modeling, Control and Applications*. John Wiley and sons Inc, 2010.

[13] A. Canelhas, S. Karamitsos, U. Axelsson, and E. Olsen, "A low frequency power collector alternative system for long cable offshore wind generation," in *11th IET Int. Conf. AC DC Power Transmission*, 2015, pp. 1–6.

[14] CIGRE, "Technical Brochure 556: Power System Technical Performance Issues Related to the Application of Long HVAC Cables," Tech. Rep. October, 2013.

[15] M. H. J. Bollen and S. Bahramirad, "Harmonic resonances due to transmission-system cables Key words," *Renew. Energy and Power Quality Journal (RE&PQJ)*, vol. 1, no. 12, 2014.

[16] T. Ohno, C. L. Bak, A. Akihiro, W. Wiechowski, and T. K. Sø rensen, "Derivation of theoretical formulas of the frequency component contained in the overvoltage related to long EHV cables," *IEEE Transactions on Power Delivery*, vol. 27, no. 2, pp. 866–876, 2012.

[17] L. Colla, S. Lauria, and F. M. Gatta, "Temporary Overvoltages due to Harmonic Resonance in Long EHV Cables," in *International Conference on Power Systems Transients (IPST 2007)*, 2007, pp. 1–6.

[18] S. Zhang, S. Jiang, X. Lu, B. Ge, and F. Z. Peng, "Resonance issues and damping techniques for grid-connected inverters with long transmission cable," *IEEE Transactions on Power Electronics*, vol. 29, no. 1, pp. 110–120, 2014.

[19] M. Cheah-Mane, J. Liang, N. Jenkins, and L. Sainz, "Electrical resonance instability study in HVDC-connected Offshore Wind Power Plants," pp. 1–5, 2016.

[20] R. Meere, I. Ibrahim, J. Ruddy, C. OLoughlin, and T. ODonnell, "Scaled hardware implementation of a full conversion wind turbine for low frequency ac transmission," *Energy Procedia*, vol. 94, pp. 182 – 190, 2016, 13th Deep Sea Offshore Wind R&D Conference, EERA DeepWind'2016.

[21] P. B. Wyllie, Y. Tang, L. Ran, T. Yang, and J. Yu, "Low Frequency AC Transmission - Elements of a Design for Wind Farm Connection," in *11th IET Int. Conf. AC DC Power Transmission*, vol. 1, 2015, pp. 1–5.

[22] M. B. Delghavi and A. Yazdani, "A control strategy for islanded operation of a distributed resource (DR) unit," *2009 IEEE Power and Energy Soc. General Meeting, PES '09*, pp. 1–8, 2009.

[23] Mathworks, "Simscape Power Systems." [Online]. Available: http://uk.mathworks.com/products/simpower/

[24] N. Cunniffe, M. V. Escudero, A. Mansoldo, E. Fagan, M. Norton, and C. Ellis, "Investigating the Methodology and Implications of Implementing Long HVAC Cables in the Ireland and Northern Ireland Power System," in *CIGRE session 2016*, Paris, 2016, pp. C4–208.

[25] D. V. Hertem, O. Gomis-bellmunt, and J. Liang, *HVDC Grids For Offshore and Supergrid of the Future*. John Wiley & Sons, Ltd, 2016.

[26] X. Wang, F. Blaabjerg, and W. Wu, "Modeling and Analysis of Harmonic Stability in an AC Power-Electronics-Based Power System," *IEEE Transactions on Power Electronics*, vol. 29, no. 12, pp. 6421–6432, 2014.

[27] H. Liu and J. Sun, "Voltage Stability and Control of Offshore Wind Farms With AC Collection and HVDC Transmission," *IEEE Journal of Emerging and Selected Topics in Power Electronics*, vol. 2, no. 4, pp. 1181–1189, 2014.

Jonathan Ruddy Jonathan Ruddy graduated with B.Sc in Engineering Science and M.E in Electrical Energy Systems from University College Dublin, Ireland in 2012 and 2013 respectively. In 2017 he received a PhD in Electrical Engineering from University College Dublin. His research focused on the integration of offshore wind using low frequency AC transmission system, in particular the power electronics and control associated with offshore transmission systems. His interests are currently the integration of power electronic systems with the AC grid and the integration of large scale offshore wind.

Ronan Meere Ronan graduated with the B.E. and M.Eng.Sc (Research) degrees in Electronic Engineering from the National University of Ireland, Galway, Ireland in 2003 and 2005 respectively. In 2010, he received a PhD in Microelectronic Engineering from the Microelectronic Engineering Department University College Cork, in conjunction with the Tyndall National Institute, Cork, Ireland. His doctoral research concentrated on the design and fabrication of planar integrated magnetics for use in low power dc/dc conversion applications. From February 2010 to August 2012 he was a Lecturer in Electronic Engineering at the Athlone Institute of Technology, Ireland. In September 2012 he joined the Electricity Research Centre as a Senior Researcher in Electrical Engineering. While at UCD, Dr. Meere focused on alternative AC transmission topologies, VSC-HVDC control/demonstration and power electronics design and optimization for future offshore wind farm development. From July 2016 June 2017, Ronan seconded from UCD to Science Foundation Ireland (SFI) as a Scientific Fellow in the Pre Award Directorate. In July of 2017, Dr. Meere joined HV Operations in ESB Networks Ireland.

Cathal O'Loughlin Cathal OLoughlin was born in Dublin, Ireland, in 1968. He received a B.E. Degree in electrical engineering from University College, Dublin in 1990, and the MEngSc Degree in 1993, also from UCD. He joined Merrimack Transformers Ireland Ltd in 1993 as a design engineer where he remained until 2003. He was awarded Techstart Employee of the year 1994. After a period in non engineering work he returned in 2010 as a research assistant in a project to design, build and test a linear switched reluctance generator at the Institute of Technology, Blanchardstown, Dublin for 2 years. He then worked in Wavebob, a company involved with wave energy devices as a design engineer on the power electronics converter, for a short period and then lectured Mathematics for 1 year in the Institute of Technology, Carlow (2012-2013). He then started in his current position as a research Engineer in 2013 in the Energy Institute, UCD. His research interests are electrical machines, power electronics, Distributed Energy Resources and real time implementation.

Terence O'Donnell Terence O'Donnell received his BE in Electrical Engineering UCD in 1990. In 1995 he received his PhD degree from National University of Ireland for research in the area of Finite Element Analysis of magnetic field problems. He joined PEI (Power Electronics Ireland) Technologies in the Tyndall National Institute in Cork in 1996 as a research officer, where he worked on industrial research projects mostly in the area of magnetic component design for application in power electronic converters. In 1999 he became a senior research officer and team leader for the power electronics team with a particular research focus on integrated magnetics for low power dc-dc conversion. From 2009 to Dec 2012 he worked with Enterprise Ireland, the Irish innovation and development agency charged with the development of indigenous Irish industry. Terence joined University College Dublin in January 2013 as an Associate Professor. His current research focus is on the use of power electronics converters in power systems and in particular on the integration and interfacing of power electronics to the grid.